Rock and Soil Mechanics

Volume 41 | Issue 1 Article 5

9-23-2020

# Experimental study on shear-seepage behaviour of rock joints under constant normal stiffness

Cai-chu XIA

Qiang-feng YU

Xin QIAN

Yang GUI

*See next page for additional authors*

# Experimental study on shear-seepage behaviour of rock joints under constant normal stiffness


## Authors

Cai-chu XIA, Qiang-feng YU, Xin QIAN, Yang GUI, and Xiao-qing ZHUANG

Rock and Soil Mechanics 2020 41(1): 57−66 ISSN 1000−7598
https: //doi.org/10.16285/j.rsm.2018.7275 rocksoilmech.researchcommons.org/journal

# Experimental study on shear-seepage behaviour of rock joints under constant normal stiffness

XIA Cai-chu, YU Qiang-feng, QIAN Xin, GUI Yang, ZHUANG Xiao-qing
Department of Geotechnical Engineering, College of Civil Engineering, Tongji University, Shanghai 200092, China

**Abstract:** In order to study the shear-flow coupling characteristics of joints under constant normal stiffness (CNS) boundary condition, the shear-flow coupling tests under three different stiffness and seepage pressure settings were carried out for duplicate joint specimens with three different joint roughnesses. Meanwhile, the effects of normal stiffness, seepage pressure and joint roughness on the mechanical properties and seepage characteristics in joint shearing process were systematically analyzed. The test results indicate that the peak shear strength of joint increases with the increasing of normal stiffness, while the flow rate, equivalent hydraulic aperture and transmissivity decrease with the increasing of normal stiffness; and the flow rate of seepage through joint surfaces decreases during shearing process with the increasing of joint roughness. Similar to the three-stage change rule of joint dilatancy, three distinct stages are also observed for the flow rate, equivalent hydraulic aperture and transmissivity: rapid growth stage, slow growth stage, and stable stage. During the stable stage, the flow rate has approximately a linear relation with the variations of the normal stiffness and seepage pressure. The joints with higher roughness present lower flow rate as the seepage pressure increases.
**Keywords:** joints; shear-seepage coupling behaviour; normal stiffness; seepage pressure; joint roughness

## 1 Introduction

It is widely accepted that proper evaluating the shear behavior of rock joint plays essential role in the engineering problems such as underground excavation design in jointed rock masses, risk assessment of underground waste disposal, slope stability analysis and design of rock-socketed piles. Traditionally, the shear behavior of rock joint is mainly focused on the studies under constant normal load (CNL) boundary condition. Under the CNL boundary condition, the applied normal load on the rock joint surface is kept constant during the shearing process. In other words, the joint surface is allowed to free deformation during the shearing. Slope stability is one of the most typical CNL boundary condition. For deep underground engineering or reinforced rock slopes with rock bolts, however, the normal stress on the joint surface will change as the shearing process. In addition, the joint dilatancy will be also constrained by the surrounding rock masses. In this fashion, the boundary condition of rock joint shearing is more suitable to the constant normal stiffness (CNS) boundary condition. Many researchers[1-4] has been elaborated the importance of shear behavior under CNS boundary condition to realistically model the shear behavior of rock joints.

The presence of water in the jointed rock mass reduces the strength of the soft rock joints. For hard rocks, stress corrosion is caused at the tips of the non-consistence joint and expansion is expected due to the existence of water. In the meantime, seepage pressure is induced due to the seepage within the rock mass and thus changes the in-situ stress filed of rock masses and could further affect the deformation behavior of joint within the rock masses. According to two authoritative conclusions of the famous Malpasset dam accident, both conclusions considered that the accident is caused by the seepage of joint fractures. Induced-earthquakes resulted from the reservoir impounded, slopes are prone to landslides in rainy seasons, etc, are also related to the water pressure and seepage of joint[5]. In this consideration, study of the shear-seepage coupling characteristics of the joint has a crucial guiding role for the structural design and stability analysis of underground engineering. Early studies were mostly focused on: the descriptions of hydraulic properties such as seepage rule of rock joints and hydraulic apertures; the application and modification of the Cube theory in joint fractures[6-11]; and the hydraulic characteristics during shearing under the CNL boundary condition. Based on test data of the granite shearing-seepage and considered the influence of shear displacement on the hydraulic aperture during shearing process, Olsson et al.[12] proposed an improved model of Barton-hydraulic aperture model. Esaki et al.[13] studied the influence of dilatancy deformation on the hydraulic conductivity of joint during shearing under CNL boundary condition and found that the trend of the hydraulic conductivity coefficient was similar to that of the joint dilatancy during shearing. Lee et al.[14] found the permeability of the rock crack with relative higher roughness decayed exponentially with the increasing of stress. The joint permeability reached to a critical stable value when the shear displacement reached up to 7-8 mm. Mitani et al.[15-16] found that hydraulic conductivity decreases as increasing normal stress during shearing process. They also pointed out that there is a little influence of the inlet water pressure on the

Received: 16 December 2018 Revised: 17 June 2019
This work was supported by the National Natural Science Foundation of China (41327001, 51778475).
First author: XIA Cai-chu, male, born in 1963, PhD, Professor, Ph.D supervisor, mainly engaged in the researches of mechanical properties of rock joints, crack mechanical properties of the frozen-swelling and large deformation behavior of soft rockmass. E-mail: tjxiaccb@126.com

hydraulic conductivity during the shearing process. According to numerical modelling results, they revealed that the contact area between the upper and lower joint surfaces was reduced largely after shearing process initiation and until reached to the peak shear displacement, in which a large number of seepage channels appeared. The contact area and seepage channels remained relatively stable during the residual shearing stage. Based on the developed rock joint shear-seepage coupling test system, Xia et al.[17] obtained a set of typical relation curves between the seepage flow quantity and shear displacement of the joint specimen under different normal stresses.

The above mentioned research results are based on the seepage characteristics of rock joints under constant load boundary conditions, however, there is a certain gap between the constant load boundary conditions and the boundary conditions of the field engineering state. As the development of experimental technology, in recent years, there have been many research results on the shear characteristics of rock joints under CNS (constant normal stiffness) boundary condition. Most of the results are the direct shear characteristics of rock joint that based on the natural surface of rock joint or replicated joint surfaces under CNS boundary condition [4,18-20]. The effect of seepage pressure on the joint shearing behavior is not considered due to the limitation of the test facilities, in this consideration, research of shear-seepage coupling characteristics of joint is relatively few under CNS boundary conditions. Olsson et al.[12] improved the existing testing machine and the CNS boundary condition was realized by hydraulic spring. They studied the effect of joint roughness of granite on seepage flow under two boundary conditions: the constant normal load and constant stiffness boundary conditions. But the seepage pressure can only reach up to 0.04 MPa. Li et al.[21] studied the influence of joint contact area and the joint roughness on the rock joint transmission rate during shearing process under constant load and under constant stiffness boundary conditions. They found that a reverse changing trend between the trend of contact ratio and the trend of transmission rate. In addition, they also pointed out the effectiveness of cube law will be improved when the joint contact areas are more dispersed. Jiang et al.[22] compared and analyzed the joint hydraulic properties during the shear-seepage process under constant load and under constant stiffness boundary conditions. They found a two-phase change law that shown for the hydraulic aperture and transmittance. However, effects of the seepage pressure, joint roughness, and normal stiffness on the shear-seepage coupling behaviors are not further analyzed in their paper. Yin et al.[23] studied the variation trends of joint hydraulic characteristics during the shearing under various seepage pressure conditions. The test results only analyzed the effect of seepage pressure on the hydraulic properties of joints and did not discuss the influence of joint roughness and normal stiffness on the joint shear-seepage coupling behavior. Because of the diversity of influence factors such as seepage pressure, joint roughness, normal stiffness, and initial normal stress level, the hydraulic characteristics of rock joint are relatively complicated during shearing process. There are few studies on the shear-seepage coupling characteristics of rock joint under CNS boundary condition and there is a lacking of systematic research on the influence of normal stiffness on the shear-seepage coupling behavior. In this consideration, there is rare research that takes these influence factors into the research of shear-seepage coupling behavior systematically and comprehensively under CNS boundary condition.

In fact, constant load boundary condition can be regarded as a special case of the constant stiffness boundary condition ( $k_n = 0$ ). For the purpose of fully revealing the coupling behavior of joint shear-seepage under CNS boundary condition, based on the newly developed full rock joint shear-seepage coupling test system, this study conducted a series of laboratory test to consider the multiple influence factors such as normal stiffness, joint roughness and seepage pressure to systematically explore the hydraulic coupling characteristics of rock joint during shearing process under constant stiffness boundary conditions.

## 2 Test facilities and specimen preparation

### 2.1 Test facilities

All the laboratory tests are conducted on a rock joint full shear-seepage coupling test system, which is developed by Tongji University independently, as shown in Fig.1. This developed test system has the capacity to perform direct shear test, shear-seepage coupling test and rheological test under various boundary conditions such as the constant stiffness, constant load and constant normal displacement boundary conditions.

The maximum load in the normal and horizontal directions of this test system is 600 kN with a loading rate of 0.01-100 kN/s. The loads in both normal and shear directions are measured by the load sensors that placed on the piston rod of the actuator. All load sensors are spoke pressure sensors that are from INTERFACE US with high precision and stability.

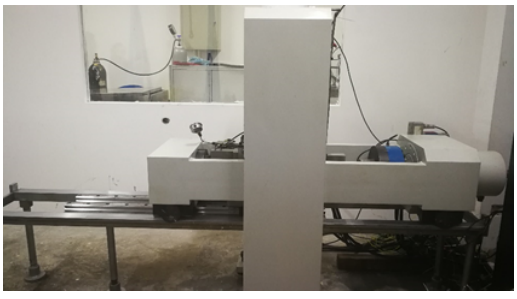

**Fig.1 Shear-seepage coupled test system for rock joints**

The shear-seepage box and its sealing system are the core of the test system, which mainly include the upper and lower shear box, lateral (side) plates of shear box, horizontal sealing strips, and sealed capsule part, etc. Under the precondition of ensuring accuracy and strength, the upper and lower shear box are machined as a whole part by using stainless steel. To solve the

sealing issue of the two end sides, the horizontal sealing strips are pressured to ensure a tight and close contact between the strips and test specimen. The lateral-sealed capsule assembly is subjected to a certain level of pressure by using the hydraulic pressure servo-loading device, the lateral-sealed water bladder is in a close contact with the specimen sides and horizontal sealing strips through the rubber block under the action of oil pressure. Therefore, it realizes the lateral sealing of the joint specimen. The maximum water pressure can reach up to 3 MPa for this test system to perform the joint shear-seepage coupling tests. In the test system, the water pressure at the inlet end is adjusted using a servo-motor to drive a low-power high-pressure plunger pump to cooperate with the accumulator and damper. The water pressure is measured using a precision pressure gauge. For the outlet end of shear-seepage box, the water pressure at outlet is adjusted by pressuring the back pressure valve using water pressure servo-control loading system. The flow measurement range of the whole test system is 0-75 L/min and more details about the test system can refer to reference [24].

In this test system, the CNS boundary condition is realized through the cross-control between signals. Prior to the test, the constant normal stiffness $k_n$ is set in the control software. During the tests, the normal displacement signals are obtained by four normal displacement sensors and the signals are transmitted to the control system. Based on the four displacement signals, the normal displacement $\Delta\delta_n$ is determined as the average value after calculation. The software system feedback signal is multiplied by the normal displacement $\Delta\delta_n$ and the pre-set $k_n$ as a closed-loop feedback signal, which is used to control the normal load $P_n$. In this way, the CNS boundary condition is achieved during the shear test and Fig.2 shows the basic control principle. In Fig.2, PC means personal computer that is used to control the whole test system. The normal load increment is calculated by Eqs.(1) and (2):

$$\Delta P_n = k_n \cdot \Delta\delta_n \tag{1}$$

$$P_n(t+\Delta t) = P_n + \Delta P_n \tag{2}$$

where $k_n$ is the pre-set normal stiffness; $\Delta\delta_n$ is the normal displacement increment within $\Delta t$; $\Delta P_n$ and $P_n(t+\Delta t)$ are the normal load increment within $\Delta t$ and $t+\Delta t$.

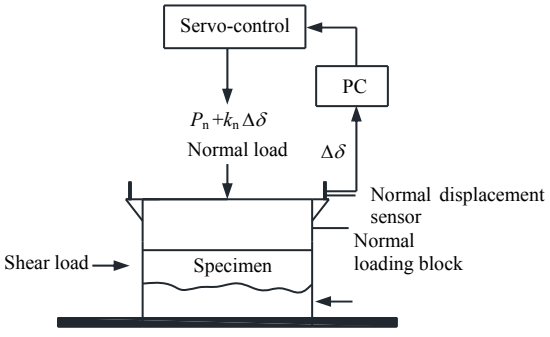


**Fig.2 Basic principle of shear test under CNS boundary condition**

### 2.2 Specimen preparation

To facilitate the quantitative analysis of the shear-seepage behavior of rock joint under different test conditions, in this study, three granite joint surfaces with various roughness were obtained using the Brazilian splitting tests. The joint surfaces were replicated using silica-gel and were numbered as RJ1, RJ2 and RJ3. The silica gel models can facilitate storage and batch copying of different joint surface for subsequent study. Fig.3 shows the three silica-gel replica joint surface models that from the splitting of granite joint. During the specimen preparation, the upper joint surface was re-engraved firstly with the silica-gel models. The upper surface was then taken as the model to replicate the lower joint surface. In this manner, a fully coupled joint surface model was then realized. The joint roughness coefficient (JRC) has been widely used in the joint researches as a parameter to denote the roughness of joint surface. The TJXW–3D portable rock 3D surface topography instrument was used to scan the rock joint herein [25] and the JRC was then determined after processing. Taking the RJ2 specimen as an example, Fig.4 shows the joint surface of RJ2 after the scanning. Through calculation [20], it was estimated that the JRCs of RJ1, RJ2 and RJ3 were in range of 6-8, 10-2 and 14-16, respectively.

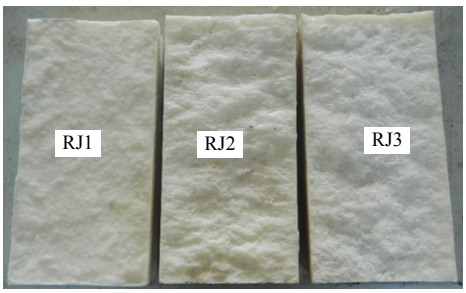


**Fig.3 Silica-gel models of rock joint**

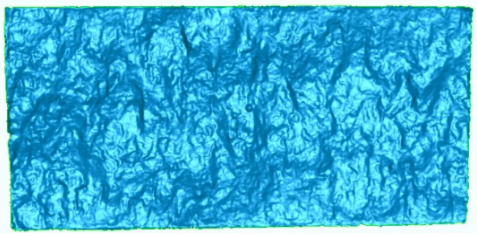

**Fig.4 RJ2 joint surface obtained after scanning**

Because of the fast setting speed and the good workability of gypsum, the gypsum is used as the raw material to make the artificial joints in this test. The specimen's dimension is 200 mm (length)×100 mm (width)×100 mm (height). The mass ratio of gypsum to water was 1: 0.28 during sample preparation. The standard specimen was tested for its compressive strength, Young's modulus and Poisson's ratio after 7 days of curing at room temperature. Table 1 shows the mechanical properties of prepared specimen.

**Table 1 Mechanical properties of specimen**

| $\sigma_t$/MPa | UCS/MPa | $E$/GPa | $\phi_b$/(° ) |
|---|---|---|---|
| 1.26±0.10 | 24.53±2.07 | 6.00±0.54 | 38.03±2.94 |

In the tests, the shear rate was set as 0.5 mm/min and the initial normal stress was set as 2 MPa. The normal stiffness was set to 0.4, 0.8, 1.6 GPa/m and the seepage pressure was set as 0.05, 0.20, 0.50 MPa. Table 2 presents the experimental cases.

**Table 2 Experimental cases of shear-seepage coupled test of joints under CNS boundary condition**

| Joint types | JRC | $k_n$ /(GPa • m$^{-1}$) | Seepage pressure /MPa | Initial normal load /MPa |
|---|---|---|---|---|
| RJ1 | 6-8 | | | |
| RJ2 | 10-12 | 0.4, 0.8, 1.6 | 0.05, 0.20, 0.50 | 2 |
| RJ3 | 14-16 | | | |

The test process is mainly divided into the following steps: (i) prior to the test, the normal load is applied first to the pre-set value level. The compressive tests are conducted before the shearing in order to make the upper and lower joint surfaces fully coupled; (ii) once the normal load is applied completely, shear displacement is applied so that the shearing loading head contacts the shear box;(iii) apply the seepage pressure to the set value and to stabilize the water pressure; (i) set up the proper corresponding normal stiffness and shear rate and can then perform the tests and record the test data.

## 3 Shear-seepage coupling test and analysis

### 3.1 Stress and displacement analysis

Fig.5 shows the shear curves for RJ1 joint under different normal stiffness when the seepage pressure and initial normal stress are set as 0.5 MPa and 2.0 MPa. It can be seen from Fig.5 that normal stiffness constrains the shear dilatancy during joint shearing test and the restriction increases as normal stress increases. In the meantime, the joint's peak shear stress and residual stress increase as the increasing of the normal stiffness under the same test conditions. In other words, existence of normal stiffness could enhance the peak and residual shear strength of the joint. Compared to the direct shear test results under the constant stiffness boundary conditions [3-4], a similar trend is identified for the effect of normal stiffness on the shear strength and normal deformation during the shear-seepage coupling tests.

Fig.6 presents the shear curves of different joint types under the conditions of $k_n$=1.6 GPa/m and $P$=0.05 MPa. It is seen that the peak shear strength and the normal displacement increase as the joint roughness increases during the shearing tests. The rougher the joints, the more asperities will be on the surface. The higher the climbing against the asperities during the shearing process, the greater dilatation will be. In addition, higher shear stress is expected due to the asperities in the shearing processing and the high peak shear strength is thus expected.

Fig.7 shows the shear curves for RJ3 joint under $k_n$ = 0.4 GPa/m and different seepage pressures. From Fig.7(a), it is seen that the shear stress decreases as the increasing of seepage pressure. This observation phenomenon can be explained according to the effective stress law of joint seepage. Based on the law of effective stress[5], assume the normal stress acting on the joint surface is $\sigma$, and the water pressure is $u$, then the shear strength of joint surface is controlled by the effective normal stress ($\sigma$–$u$). The relation between the joint shear strength and the normal stress is:

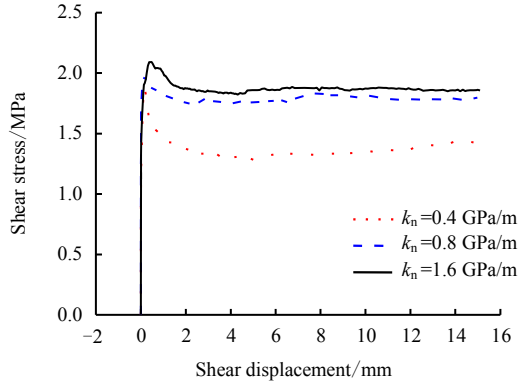


(a) Shear stress vs. shear displacement

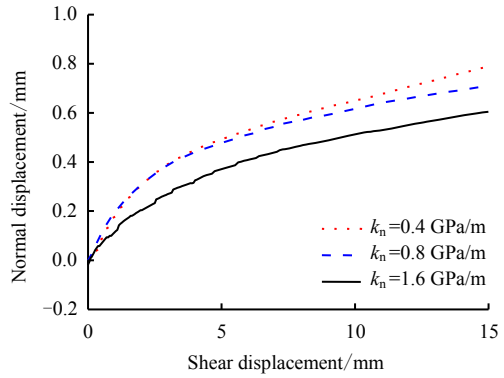


(b) Normal displacement vs. shear displacement

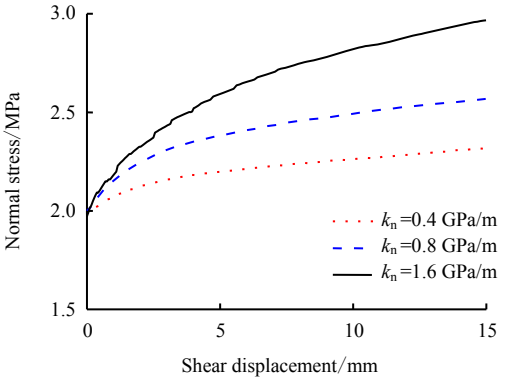


(c) Normal stress vs. shear displacement

**Fig.5 Shear curves of joints with different normal stiffness (RJ1, $P$=0.50 MPa)**

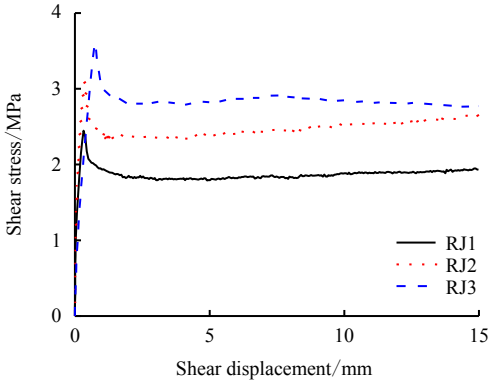


(a) Shear stress vs. shear displacement

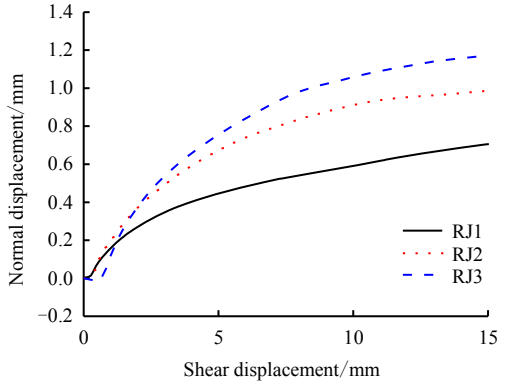


(b) Normal displacement vs. shear displacement

**Fig.6 Shear curves of joints with different roughness ($P$=0.05 MPa，$k_n$=1.6 GPa/m)**

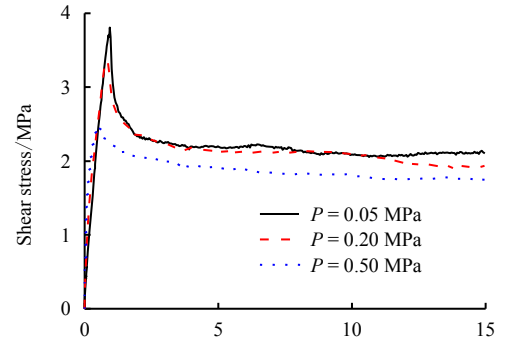


(a) Shear stress vs. shear displacement

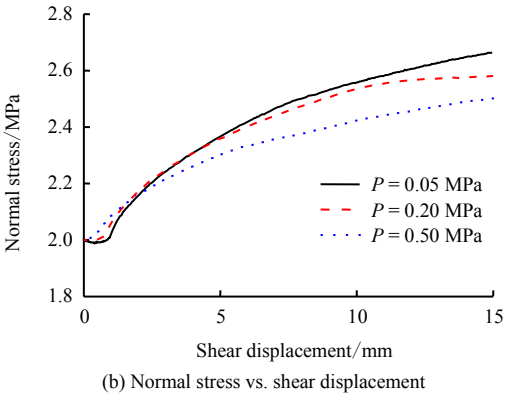


(b) Normal stress vs. shear displacement

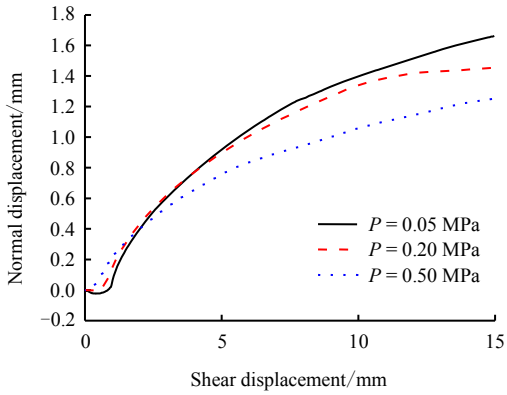


(c) Normal displacement vs. shear displacement

**Fig.7 Shear curves of joints with different seepage pressures (RJ3, $k_n$=0.4 GPa/m)**

$$\tau = c + (\sigma - u)\tan\varphi \tag{3}$$

where $\tau$ is the shear strength; $c$ is the cohesion of rock mass and $\varphi$ is the friction angle.

In Eq.(3), considering the fact that both cohesion $c$ and friction angle $\varphi$ of most hard rocks do not change significantly due to influence of water content, it is therefore considering that the reducing of the effective normal stress $\sigma$–$u$ is the main reason that caused the decreasing of shear strength [5]. With the increasing of seepage pressure, the effective normal stress is then reduced at the joint surface and thus leads to the reducing of shear strength of joints. From Fig.7(b), it is also seen from the normal stress change that the smaller the seepage pressure, the higher the normal stress that acting on the joint surface. When the seepage pressure is 0.5 MPa, the shear strength has an obvious decreasing trend, which indicates that the weakening effect of seepage pressure on shear strength becomes more obvious as the increasing of seepage pressure.

Fig.7(c) shows the curves between the shear displacement and normal displacement under different seepage pressures. It is seen that the dilatancy decreases as the seepage pressure increases. Theoretically, the dilatation should be increase as increasing of seepage pressure due to the reduction of effective normal stress at the joint surface under the constant load boundary condition. Under constant stiffness boundary condition, however, the increasing of dilatancy would result in the increasing of normal load at the joint surface, which would in turn constraints the joint dilation. Under the same conditions, the increasing trend of joint normal displacement becomes obvious as the seepage pressure increases. Meantime, the restriction effect of normal stiffness on the normal displacement also becomes obvious. It is hence found that the normal stress and normal shear dilatancy show decreasing trend even under high seepage pressure conditions.

### 3.2 Flow rate analysis

The flow rate is the velocity of the fluid flowing through the joint surface during the shearing process. The fluid flow affects the stress field that acting on the joint surface and thus influence the hydraulic behavior during the shearing. Fig.8(a) shows the flow rate curves for RJI joint under different normal stiffness and 0.5 MPa seepage pressure. As mentioned in the Section 3.1, the normal stiffness contains the normal dilation during the joint shearing test. A higher stiffness means a smaller dilation, which leads to a relatively narrow flow path for the water passing. Hence, the normal stiffness affects the flow rate by affecting the joint dilatancy during the shearing process. It is seen from Fig.8(a) that the joint flow rate decreases as the normal stiffness increases under the same seepage pressure conditions.

Fig.8(b) presents the relations between the flow rate and shear displacement for RJ2 joint under $k_n$ = 0.8 GPa/m and different seepage pressure conditions. Seepage pressure is one of the most important factors that affect the flow rate. Form Fig.8(b), it is found that the flow rate increases as the increasing of the seepage pressure. Comparing the change trend of the flow rate under various seepage pressures, it is seen that a large variation of flow rate is resulted from the seepage pressure.

When the tests reach a stable state, the flow rate difference can reach up to 20 times when comparing the flow rate of 0.50 MPa seepage pressure with that from the 0.05 MPa seepage pressure.

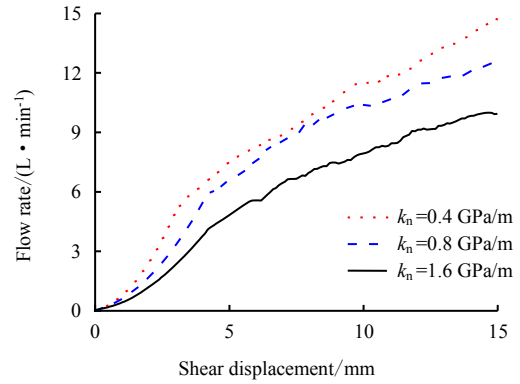


(a) Flow rate vs. shear displacement under different normal stiffness (RJ1, $P$ =0.50 MPa)

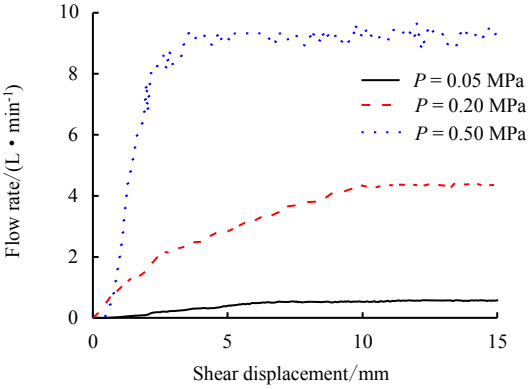


(b) Flow rate vs. shear displacement under different seepage pressures (RJ2, $k_n$ =0.8 GPa/m)

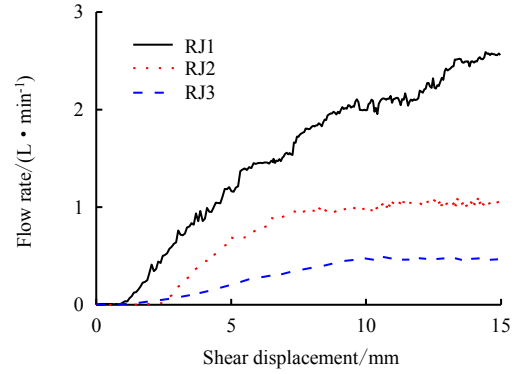


(c) Flow rate vs. shear displacement under different roughness ($k_n$ =0.8 GPa/m, $P$ =0.05 MPa)

**Fig.8 Results of flow rate test**

Fig.8(c) illustrates the relations between the flow rate and shear displacement under different joint roughness. In the shear-seepage coupling tests, the joint dilatancy increases as the joint roughness increases during the shearing process. Among the all testing joints, RJ3 joint shows the maximum dilation during the shearing process under the same experimental conditions. Theoretically, the flow rate should be also increased due to the large dilation of RJ3 joint. Based on test results, however, it is found that the rougher joint associates with small flow rate. For instance, the RJ1 joint with smallest roughness has the maximum flow rate during the shearing. This phenomenon could be explained from the following two aspects: on the one hand, referring to the coupled joint, the smoother the joint surface, the smoother the water flow through the joint surface is. On the contrary, the rougher the joint surface, the tighter the upper and lower joint surfaces is and the larger the contact areas between the asperities, which reduces the water channels of flow path and thus reduces the flow rate. In the meantime, for rougher joint, more rock debris will be generated during the shearing process, which increases the resistance to the water flow; on the other hand, more tortuous flow paths will be formed in the joint surface with higher roughness. The tortuous flow paths would cause the vortex phenomena, which could lead to energy losing and the water head is consumed without any contributions to the effluent flow. Although the normal dilation is larger, the water flow rate is relatively small. In the meantime, it is found that the low-roughness RJ1 joint has the fastest flow growth rate during the shearing process and it reached to a stable value after a relatively long shear displacement.

When comparing the flow changes during the tests in Fig.8, it is observed that the flow rate through the joint surface can be divided into three stages: (i) the rapid growth stage, where the flow rate growth rate is becoming faster and faster; (ii) the slow growth rate stage, where the flow rate growth rate tends to be slow down and gradually reaches to zero and the flow rate finally reaches to a stable value; (iii) the stable stage, where the flow rate tends to be stable and basically no longer changes. Due to the low roughness of RJ1 joint in Fig.8(a), a relatively large shear displacement is required to reach to the stable stage. At this time, the shear displacement is about 15 mm and it has not yet entered to the stable stage during the shearing.

From the above analysis, it is found that the flow rate will eventually reach to a stable stage with the shearing process. Within this stable stage, the flow rate only fluctuates within a very small range, but it is affected by various conditions such as joint roughness, seepage pressure and normal stiffness. According to the test results, the time for joints to reach the stable state is different during the shearing. It should be bear in mind that the shear rate is constant during the shearing test. The time that required to reach stable state can be then estimated based on the shear displacement and shear rate. For RJ1 joint under $k_n$ = 0.8 GPa/m and $P$ = 0.5 MPa in Fig.8, the flow rate is about 10 L/min within the stable state, the time is then calculated about 30 min to reach to the stable state. Fig.9 shows the variations of flow rate with different seepage pressures in stable stage under the same normal stiffness and same initial normal stress. Under the same test conditions, it can be seen from Fig.9 that the flow rate increases as the seepage pressure increases in the stable stage for joints with different roughness. The flow rate changes approximately linearly with the seepage pressure. According to the slope of the flow rate change with the seepage pressure, the low-roughness RJ1 has the maximum growth rate of flow rate during the shearing, while the high-roughness RJ3 has the lowest flow growth rate, which means the lower the joint roughness is, the faster the flow

growth rate will be. This mainly occurs in the stable stage. Due to the failure of asperities during the shearing, the entire joint surface is then relatively smooth. The main factor affecting the joint seepage is the debris from the asperities shearing. Large number of asperity is normally associated with the high-roughness joint and lots debris will be formed during the shearing process, which leads to large contact areas and a long tortuous path for fluid flow and thus inhibits the fluid flow velocity to certain extent.

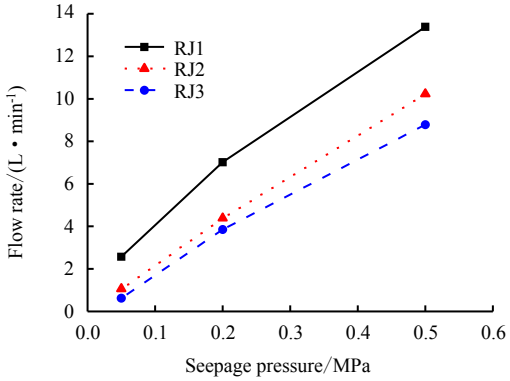


(a) $k_n$=0.8 GPa/m

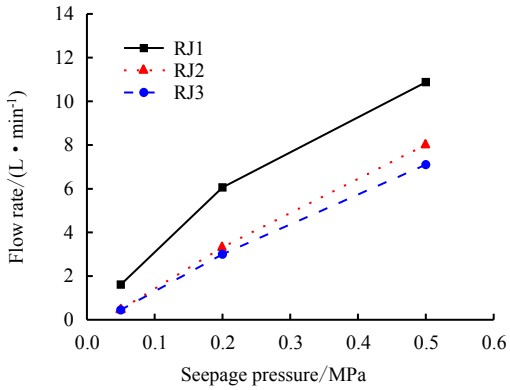


(b) $k_n$=1.6 GPa/m

**Fig.9 Variations of flow rate with seepage pressure in stable stage**

Under constant stiffness boundary conditions, the normal stiffness mainly affects the flow rate by affecting the joint dilatancy during the joint shearing process. Fig.10 presents the variations of flow rate with different normal stiffness in stable stage. Under the same test conditions, it can be seen from Fig.10 that there is a linear relation between the flow rate and the normal stiffness. Comparing the test results of the flow rate change with the normal stiffness in the stable stage in Fig.10, as the increasing of normal stiffness, relatively low-roughness RJ1 joint has higher flow rate when compared that with the RJ2 and RJ3 joints under the same seepage pressure and normal stiffness. This is caused by the relatively fewer asperities on the RJ1 joint surface and a smoother flow path is formed for the water flow passing. On the contrary, greater obstacles will be formed for the high-roughness joints. In addition, the flow rate difference is relatively small between the RJ2 and RJ3 joints and the difference decreases gradually with the normal stiffness increases. When the normal stiffness is 1.6 GPa/m, the difference of flow rate between the two joints almost disappears, which is because the difference of dilatancy decreases as the increasing of the normal stiffness for different types of joints during the shearing process. In the meantime, the two joints are relatively rough and thus have more zigzag flow paths, which will reduce the channels for water passing.

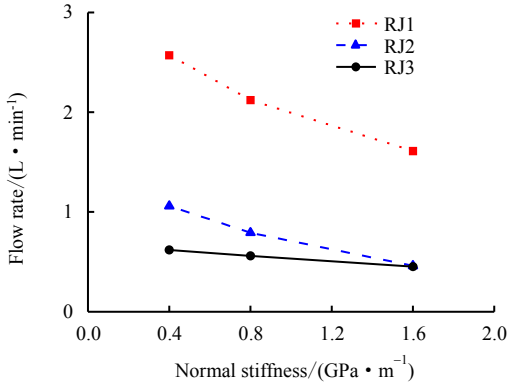


(a) $\sigma_{n0}$=2 MPa, $P$=0.05 MPa

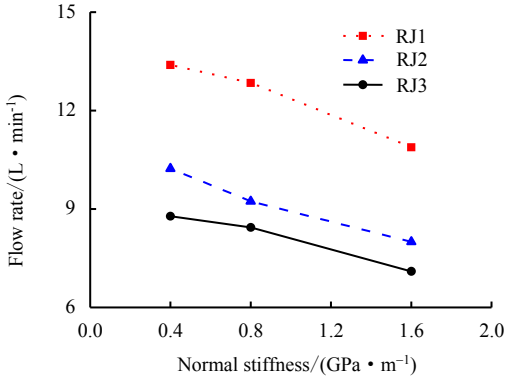


(b) $\sigma_{n0}$=2 MPa, $P$=0.5 MPa

**Fig.10 Variations of flow rate with normal stiffness in stable stage**

### 3.3 Equivalent hydraulic aperture analysis

Water seepage within joint is closely related to the joint opening degree, surface morphology and contact stage of joints. It is difficult to describe the rock joint permeability behavior accurately due to the complexity arisen from the joint roughness and the contact areas between joint surfaces. The water flow states within joints normally include the laminar state, transition state and turbulent state. Firstly, the seepage state is assumed as the laminar state with an aperture of $e$ and the surface is smooth and infinitely extended. The joint length is far greater than its width. The joint can then be regarded as a parallel plate-shaped slit and the seepage law of water in the joint is:

$$Q=\frac{gwe^3}{12v}i \tag{4}$$

where $Q$ is the water seepage flow; $g$ is the gravity acceleration; $v$ is the dynamic viscosity coefficient; $w$ is the width of the flow area and $i$ is the unit hydraulic gradient.

Because the flow rate is proportional to the cube of the joint aperture $e$ in Eq.(4), it is called the cube law. It should be mentioned that the cubic theorem describes joint seepage on the precondition that the joint is smooth and straight without any

fillings. However, natural joints are not completely smooth and straight and often have complex material components, structures and physical properties. Cook et al.[26] pointed out that the cube theorem only approximates the seepage law of joints with smooth and straight sides, large aperture and without any fillings. When the normal stress on the joint is greater than 10 MPa, the cubic theorem cannot be applied. In this manner, the hydraulic aperture estimated from the cubic theorem is an equivalent hydraulic aperture.

Fig.11(a) shows the relationships between the equivalent hydraulic aperture and the shear displacement under different normal stiffness and under 0.5 MPa seepage pressure for RJ1 joint. Under the same test conditions, it can be seen from Fig.11(a) that the equivalent hydraulic aperture decreases as the normal stiffness increases during the shearing process. In the meantime, the equivalent hydraulic opening value (Fig.11(a)) and the normal displacement value (Fig.5(b)) of RJ1 joint under the condition of normal stiffness of 0.4GPa/m and 0.5 MPa water pressure are compared. It is found that the stable equivalent hydraulic aperture is 0.22 mm, while the peak normal displacement is about 0.80 mm, which indicates that there is a large difference between the equivalent hydraulic aperture and the normal displacement. This difference is mainly due to the cubic law assuming that the joint surfaces are smooth and straight, however, in the actual shearing process, the upper and lower joint surface are interacted in contact each other and there are debris due to the shearing. It is therefore to have a large difference between the normal displacement obtained in the tests and the equivalent hydraulic aperture obtained by the cube law calculations.

Fig.11(b) gives the relationships between the equivalent hydraulic aperture and the shear displacement under different seepage pressures and under $k_n$ = 0.8 GPa/m. For the same joint and based on cubic law calculation, it is found from Fig.11(b) that the equivalent hydraulic aperture increases as the seepage pressure increases. However, when compared with the flow rate difference caused by different seepage pressures, the equivalent hydraulic aperture calculated by the cubic law is relatively small. This is because the larger the seepage pressure is, the larger the hydraulic gradient is. In the calculation, the increment of hydraulic gradient greatly reduces the difference in the equivalent hydraulic aperture that caused by the flow rate difference.

Fig.11(c) presents the relationships between the equivalent hydraulic aperture and the shear displacement under different roughness. After the equivalent hydraulic aperture tends to be stable, the equivalent hydraulic aperture decreases as the increasing of the joint roughness. When comparing the test results of the equivalent hydraulic aperture change under different test conditions, it is found that there are three phases that similar to the three stages of flow rate change during the whole shearing process. They are: the rapid growth stage, the slow growth stage and the stable stage.

### 3.4 Transmittance change analysis

In shear-seepage coupling test, the transmittance denotes the difficulty extent of water flowing through the joint during shearing. The relation between the transmissivity and the shear displacement, to some extent, reflects the shear-seepage coupling behavior of the specimen. The transmittance is calculated by:

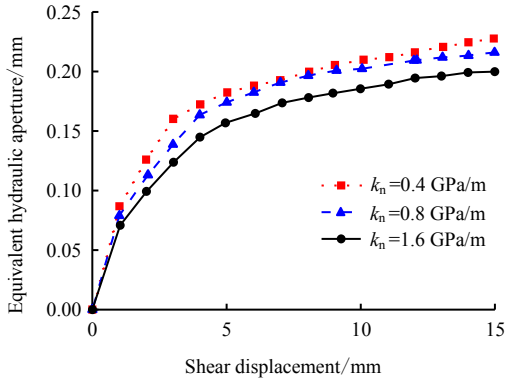


(a) Equivalent hydraulic aperture vs. shear displacement under different normal stiffness (RJ1, $P$ =0.5 MPa)

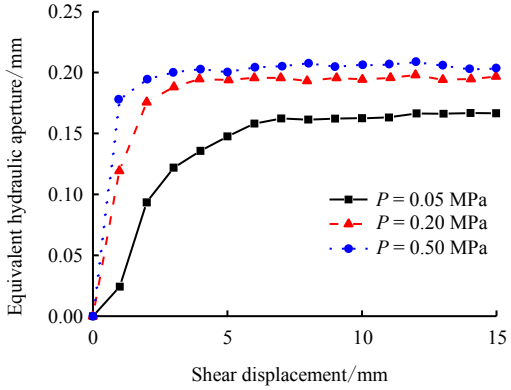


(b) Equivalent hydraulic aperture vs. shear displacement under different seepage pressures (RJ2, $k_n$ =0.8 GPa/m)

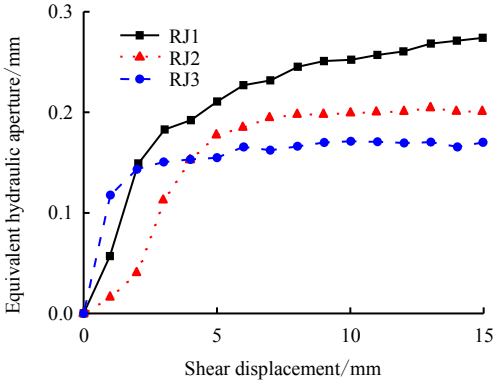


(c) Equivalent hydraulic aperture vs. shear displacement under different roughness ($k_n$=0.8 GPa/m，$P$ =0.05 MPa)

**Fig.11 Results of equivalent hydraulic aperture test**

$$T = \frac{Q}{wi} \tag{5}$$

where $T$ is the water transmittance.

Fig.12(a) shows the relation curves between the transmittance and shear displacement under different normal stiffness conditions. It is seen that the transmittance decreases as increasing of the normal stiffness during the joint shearing. A larger decreasing extent of transmittance is observed at a greater normal stiffness condition. Compared with the two normal stiffness cases of 0.4 GPa/m and 0.8 GPa/m, the joint transmittance shows a rapidly decreasing for the normal

stiffness case of 1.6 GPa/m. Fig.12(b) and Fig.12(c) present the comparison results of the joint transmittance under different seepage pressures and different joint roughness conditions. Under the same test conditions, it is seen that the transmittance increases as the seepage pressure increases. Besides, the transmittance decreases as the roughness increases. In addition, the transmittance of low-roughness joint has a relatively fast growth rate during the whole shearing process and requires a relatively larger shear displacement in order to reach the stable stage.

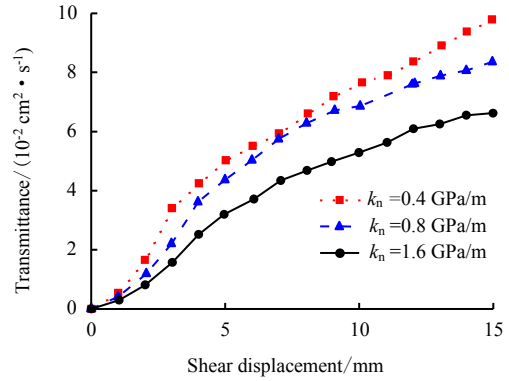


(a) Transmittance vs. shear displacement under different normal stiffness (RJ1, $P$ =0.5 MPa)

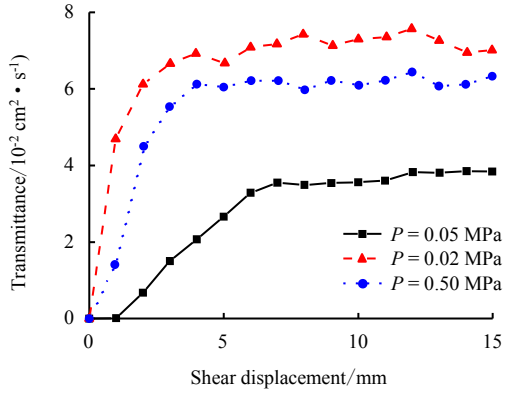


(b) Transmittance vs. shear displacement under different seepage pressures (RJ2, $k_n$ =0.8 GPa/m)

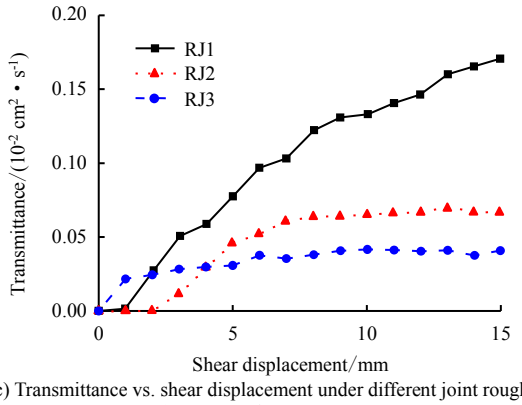


(c) Transmittance vs. shear displacement under different joint roughness ($k_n$ =0.8 GPa/m, $P$ =0.05 MPa)

**Fig.12 Test results of transmittance**

Esaki et al. [13] found that the variation trend of hydraulic conductivity was similar to that of joint dilatancy during the shearing. Comparing the change rules of the transmittance with the shear displacement under different test conditions in Fig.12 and the test results of flow rate and equivalent hydraulic aperture in Section 3.3, it is found that the change trends of flow rate, equivalent hydraulic aperture and transmittance with the shear displacement also show three stages under different conditions, which is similar to the three stages of the normal displacement. The three stages are: (i) the rapid growth stage, where the transmittance growth rate is fast and this stage corresponds to the rapid growth stage of normal dilatation; (ii) the slow growth rate stage, where the joint asperities gradually breaks down and the growth rate of normal dilation decreases gradually. The growth rate also decreases gradually and finally reaches to zero; (iii) the stable stage, where the dilation tends to be stable and all the tree hydraulic parameters tend to be stabilized.

## 4 Conclusions

In this paper, experimental tests were conducted to study the shear-seepage coupling behavior of rock joint under constant normal stiffness (CNS) boundary condition considering various influence factors such as normal stiffness, joint roughness and seepage pressure. The coupling relation between the joint mechanical properties and seepage characteristics is qualitatively analyzed. After the shear deformation under the action of shear force, the joint aperture changes and thus affects the normal stress on the joint faces. The normal stress in turn constrains the normal dilation during the shearing process. In addition, the effective normal stress is also affected by seepage pressure. Factors such as normal stiffness, seepage pressure and joint roughness influence each other and thus affect the hydraulic behavior during the shearing process. The main conclusions are:

(1) The peak and residual shear strength of joint increase as the increasing of the normal stiffness. The restriction of the normal stiffness on the joint dilation increases as the normal stiffness increases. The flow rate, equivalent hydraulic aperture and transmittance through the joint surface decrease with the normal stiffness increases.

(2) The seepage pressure affects the hydraulic behavior of the joint shearing process by affecting the effective normal stress that acting on the joint surface. The joint peak shear strength and normal displacement decrease as the seepage pressure increases. The flow rate, equivalent hydraulic aperture and transmittance increase as the increasing of the seepage pressure. Besides, the equivalent hydraulic aperture is much smaller than the normal displacement.

(3) Because the influence of joint contact areas, rock debris and vortex phenomenon, the flow rate, equivalent hydraulic aperture and transmittance decrease as the joint roughness increases. The low-roughness joints have the fastest flow growth rate during the shearing process and require a relatively long shear displacement to reach the stable value.

(4) During the joint shear-seepage coupling test process, the change trends of the flow rate, equivalent hydraulic aperture and transmittance show three stages similar to the three stages of the joint dilatation. The three stages are: a) the rapid growth stage, where the increasing at a large growth rate and this stage corresponds to the rapid growth stage of normal dilatation; b) the slow growth rate stage, where the joint asperities gradually

breaks down and the growth rate of normal dilation decreases gradually. The growth rate also decreases gradually and finally reaches to zero; c) the stable stage, where the dilation tends to be stable and the flow rate, equivalent hydraulic aperture and transmittance tend to be stabilized. During the stable stage the flow rate has approximately a linear relation with the variations of the normal stiffness and seepage pressure. As the normal stiffness increases, the difference in flow rate decreases gradually among different types of joint. In the meantime, the joints with higher roughness present lower flow growth rate as the increasing of the seepage pressure.

## References

[1] HEUZE F E. Dilatant effects of rock joints [C]//4th ISRM congress. Montreux: [s. n.], 1979.

[2] JOHNSTON I W, LAM T S K, WILLIAMS A F. Constant normal stiffness direct shear testing for socketed pile design in weak rock[J]. Geotechnique, 1987, 37(1): 83-89.

[3] SHRIVASTAVA A K, RAO K S. Shear behaviour of rock joints under CNL and CNS boundary conditions[J]. Geotechnical and Geological Engineering, 2015, 33(5): 1205-1220.

[4] INDRARATNA B, HAQUE A. Experimental study of shear behavior of rock joints under constant normal stiffness conditions[J]. International Journal of Rock Mechanics and Mining Sciences, 1997, 34(3): 141. e1-e14.

[5] XIA Cai-chu, SUN Zong-qi. Jointed rock mechanics of engineering rock[M]. Shanghai: Tongji University Press, 2002: 141.

[6] BARTON N. Modelling rock joint behavior from in situ block tests: implications for nuclear waste repository design[M]. [S. l.]: [s. n.], 1982.

[7] XIA Cai-chu, WANG Wei, CAO Shi-ding. Flow characteristics of joints under different contact conditions[J]. Chinese Journal of Rock Mechanics and Engineering, 2010, 29(7): 1297-1306.

[8] TSANG Y W, WITHERSPOON P A. The dependence of fracture mechanical and fluid flow properties on fracture roughness and sample size[J]. Journal of Geophysical Research, 1983, 88(B3): 2359-2366.

[9] ZHOU Chuang-bing, XIONG Wen-lin. A generalized cubic law for percolation in rock joints[J]. Rock and Soil Mechanics, 1996, 17(4): 1-7.

[10] SU Bao-yu, ZHAN Mei-li, ZHAO Jian. Study on fracture seepage in the imitative nature rock[J]. Chinese Journal of Geotechnical Engineering, 1995, 17(5): 19-24.

[11] AMADEI B, ILLANGASEKARE T. A mathematical model for flow and solute transport in non-homogeneous rock fracture[J]. International Journal of Rock Mechanics and Mining Sciences & Geomechanics Abstracts, 1994, 31(6): 719-731.

[12] OLSSON R, BARTON N. An improved model for hydromechanical coupling during shearing of rock joints[J]. International Journal of Rock Mechanics and Mining Sciences, 2001, 38(3): 317-329.

[13] ESAKI T, DU S, MITANI Y, et al. Development of a shear-flow test apparatus and determination of coupled properties for a single rock joint[J]. International Journal of Rock Mechanics and Mining Sciences, 1999, 36(5): 641-650.

[14] LEE H S, CHO T F. Hydraulic characteristics of rough fractures in linear flow under normal and shear load[J]. Rock Mechanics and Rock Engineering, 2002, 35(4): 299-318.

[15] MITANI Y, SHARIFZADEH M, ESAKI T, et al. Development of shear-flow test apparatus and determination of coupled properties of rock joint[C]// International Symposium of the International Society for Rock Mechanics, EUROCK 2005. Brno: [s. n.], 2005.

[16] MITANI Y, ESAKI T, IKEMI H, et al. Numerical examination of flow mechanism during shear in a rock joint[C]//11th ISRM Congress. Lisbon: [s. n.], 2007.

[17] XIA Cai-chu, WANG Wei, WANG Xiao-rou. Development of coupling shear-seepage test system for rock joints[J]. Chinese Journal of Rock Mechanics and Engineering, 2008, 27(6): 1285-1291.

[18] JOHNSTON I W, LAM T S K. Shear behavior of regular triangular concrete/rock joints—analysis[J]. Journal of Geotechnical Engineering, 1989, 115(5): 711-727.

[19] JIANG Y, XIAO J, TANABASHI Y, et al. Development of an automated servo controlled direct shear apparatus applying a constant normal stiffness condition[J]. International Journal of Rock Mechanics and Mining Sciences, 2004, 41(2): 275-286.

[20] SHRIVASTAVA A K, RAO K S. Shear behaviour of rock joints under CNL and CNS boundary conditions[J]. Geotechnical and Geological Engineering, 2015, 33(5): 1205-1220.

[21] LI B, JIANG Y, KOYAMA T, et al. Experimental study of the hydro-mechanical behavior of rock joints using a parallel-plate model containing contact areas and artificial fractures[J]. International Journal of Rock Mechanics and Mining Sciences, 2008, 45(3): 362-375.

[22] JIANG Yu-jing, WANG Gang, LI Bo, et al. Experiment study and analysis of shear-flow coupling behaviors of rock joints[J]. Chinese Journal of Rock Mechanics and Engineering, 2007, 26(11): 2253-2259.

[23] YIN Li-ming, CHEN Jun-tao. Experimental study of influence of seepage pressure on joint stress-seepage coupling characteristics[J]. Rock and Soil Mechanics, 2013, 34(9): 2563-2568.

[24] XIA Cai-chu, QIAN Xin, GUI Yang, et al. A novel multi-functional shear-flow coupled test system for rock joints and its application[J]. Chinese Journal of Rock Mechanics and Engineering, 2007, 26(11): 2253-2259.

[25] XlA Cai-chu, WANG Wei, DING Zeng-zhi. Development of three dimensional TJX-3D-typed portable rock surface topography[J]. Chinese Journal of Rock Mechanics and Engineering, 2008, 27(7): l285-1291.

[26] COOK N G W. Natural joints in rock: mechanical, hydraulic and seismic behaviour and properties under normal stress[J]. International Journal of Rock Mechanics and Mining Sciences & Geomechanics Abstracts, 1992, 29(3): 198-223.